



# Propeller and Wave-Induced Hull Structure Vibrations

S. G. Stiansen, Member, American Bureau of Shipping,  
New York, New York

## ABSTRACT

The American Bureau of Shipping has investigated propeller-induced and wave-induced hull structure vibrations on many types of vessels to ensure compliance with strength standards and specified habitability criteria. This paper illustrates some large-scale vibration analyses performed with the aid of finite element computer models representing entire vessels. The analyses provide detailed information on frequencies and response of deckhouses, shafting and other critical areas to propeller-induced forces. Modeling techniques, together with their application and influence on results, are discussed.

The paper also describes the vibratory response of ship hulls to the excitation of irregular wave loads. This phenomenon includes the so-called "springing" coupled with the wave-induced bending moment in a random process which can be represented mathematically with a flexible beam model.

Correlation between calculated results and data from full-scale measurements is presented and evaluated. Some of the potential problems caused by vibrations are discussed, together with proposed feasible solutions.

## NOMENCLATURE

$A_B$	column cross-sectional area
$B$	subscript denoting equivalent bar
$B_i$	breadth of ship at waterline
B.R.	blade rate
(C)	damping matrix
$C_s$	scattering parameter
$c$	combined stress
$D$	density of water
$E_B$	column modulus of elasticity
$H_{1/3}$	significant wave height

$i$	subscript denoting ship station
(K)	stiffness matrix
$K_B$	column stiffness
$K_i$	vertical buoyancy stiffness
$L$	longitudinal direction
$L_B$	column length
$L_i$	spacing between ship stations
(M)	mass matrix
$N$	number of stress records
$r_o$	radius of propeller
RAO	response amplitude operator
RMS	root-mean-square
$s$	springing stress
$V$	vertical direction
$w$	low-frequency wave-induced stress
$\alpha$	mass damping coefficient
$\beta$	stiffness damping coefficient
$\zeta$	ratio of actual to critical damping
$\omega$	natural frequency
$2 \times \text{B.R.}$	twice blade rate

## INTRODUCTION

The problem of ship vibrations has existed for a long time, but its severity has been increased recently by the trend towards vessels of greater power and higher speed. The vibration problems refer to the structure of the ship and its components. The necessity of avoiding excessive deflections and stresses in the ship's structure and its components, as well as the comfort required by a ship's crew and the smooth rides required by delicate onboard instruments have underlined the importance of ship vibrations. Accordingly, many investigations of an analytical and/or empirical nature have been conducted in the last decade to gain a better understanding of the various phases of ship vibrations, their

causes, their effects, and the most effective ways to minimize the problems that they bring about. The main purpose of these investigations is to develop analytical tools which can be used to eliminate potential problems at an early design stage.

A first step in the solution of a complex problem with many variables is to separate the variables and study their individual effects on the overall result. Then the variables can be categorized by their proper importance and influence on the overall results. The last step is to combine as many variables as are necessary to obtain realistic values of the desired solutions.

This has been the approach summarized in this paper, which describes some of the results obtained at the American Bureau of Shipping during the course of numerous investigations into different aspects of ship vibrations. The examples presented are illustrative rather than comprehensive and indicate further areas where additional research is advisable.

#### PRELIMINARY CALCULATIONS

##### Propeller Forces

As the ship operates in the sea, there are various sources of periodic excitation forces which may excite ship vibration. However, the propeller-induced vibratory forces remain the most important of all periodic forces, especially since the trend in shipbuilding is toward high-power flexible ships.

The following discussion refers to generalized forces, i.e. forces and moments.

The propeller-induced vibratory forces may be transmitted to the hull in two distinctly different ways:

- 1) Directly through the shafting bearings, the so called "bearing forces."
- 2) Indirectly by way of the unsteady water pressure field acting on the surface of the stern counter, the so-called "surface forces."

The "bearing forces" are due entirely to the circumferential non-uniformity of the hull wake. The "surface forces" depend on the circumferential

non-uniformity of the hull wake as well as propeller blade cavitation, which in many instances is the dominant factor that causes severe ship vibration.

The propeller-induced vibratory forces can be calculated by a program such as ABS/SURFORCE, for which the hull geometry, ship speed, hull wake, propeller geometry, RPM and cavitation characteristics must be given.

The hull geometry is defined by contour lines at various longitudinal stations (see Figures 1 and 2). Finer-spaced stations should be used in the stern region to get a better degree of accuracy in the calculation. The propeller geometry is usually modeled by equally-spaced radial stations, and at each station, the propeller section geometry (wing section) is represented by equally-spaced offsets, as shown in Figure 3. The required hull wake data is usually taken from a wake experiment.

The cavitation pattern can be modeled from propeller tests in a cavitation tunnel, as illustrated in Figure 4. The "sheet" cavitation has been found to be the predominant source of cavitation-induced "surface force". The cavitation pattern can be described by the extent of cavitation, the inception angle and termination angle of cavitation, and the rates of developing and collapsing of cavitation.

By assuming a linear theory, the propeller-induced perturbation to the flow may be regarded as a superposition of the effect of the blade pressure "loading" (due to the shape of propeller camber), and the fluid displacing effect of the blade "thickness." The bearing forces are due to the "loading" effect only. The "surface forces" are caused by both "loading" and "thickness" effects. When the propeller is cavitating, it produces an additional "thickness" effect. Bearing and surface forces are usually calculated at blade rate and twice blade rate since higher frequency components are negligible. To illustrate the individual relative magnitudes of these forces, the bearing forces and vertical surface forces for a medium-size tanker are shown in Table I.

Both the magnitude and the phase angle (position of the propeller blade nearest top-dead-center when the vertical upward force is maximum) of all the

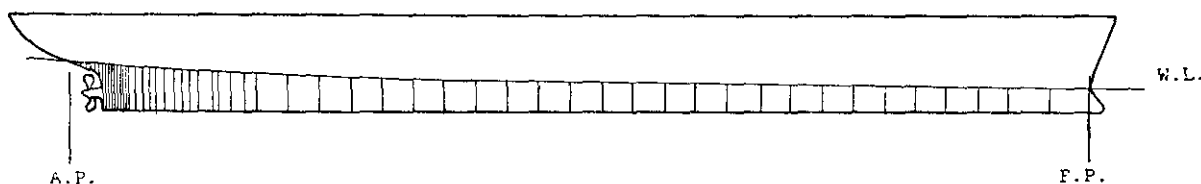


Fig. 1 Longitudinal stations for calculations of added mass and propeller-induced vibratory forces

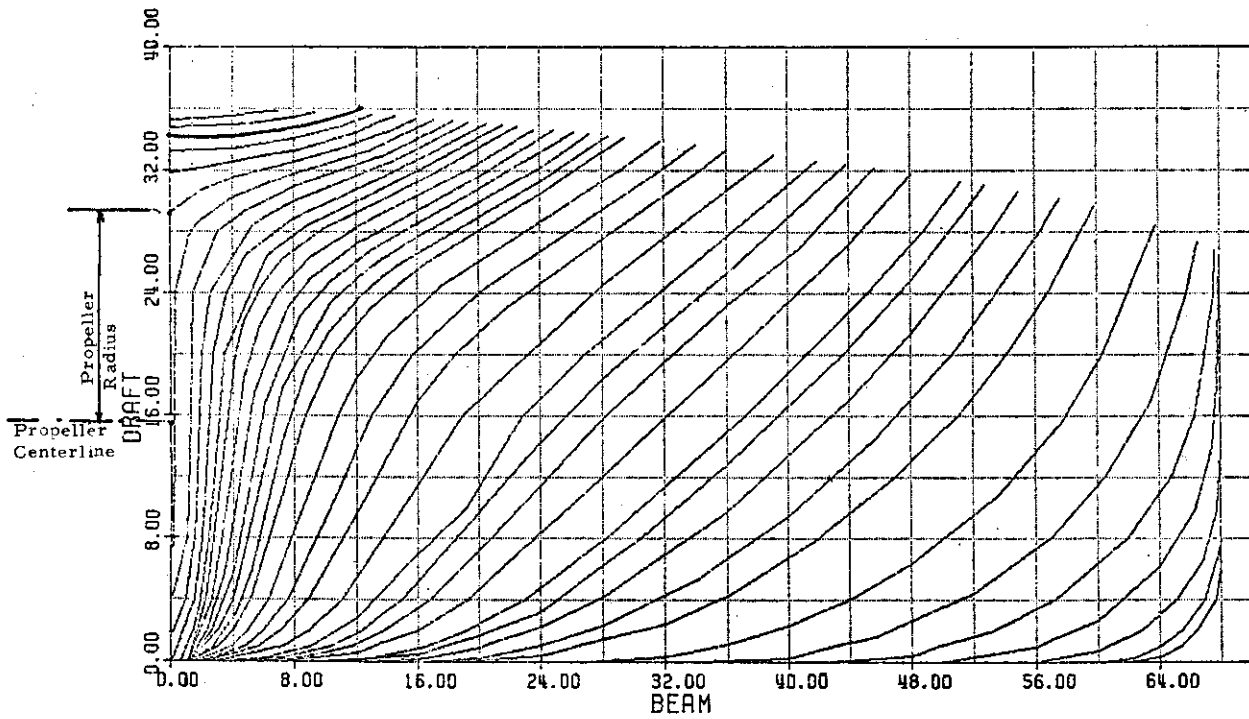


Fig. 2 Body plan

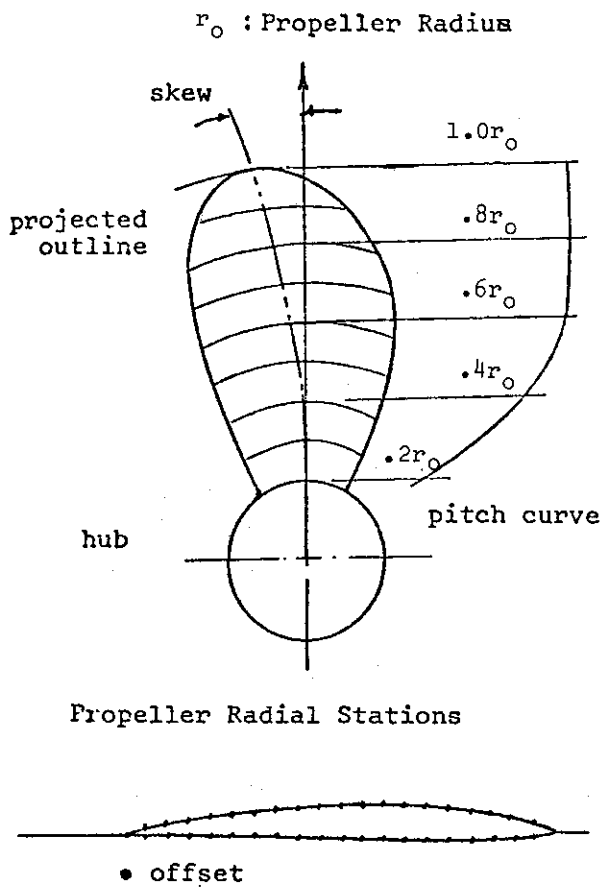


Fig. 3 Propeller radial stations and offsets

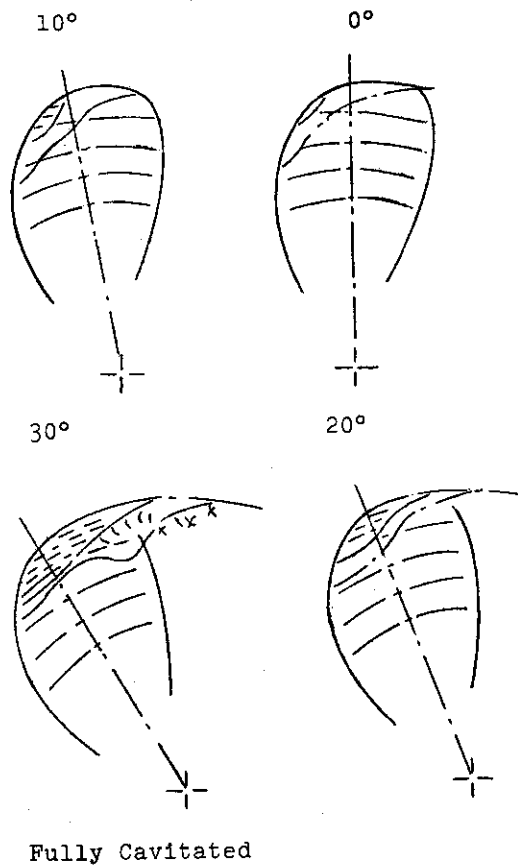


Fig. 4 Propeller cavitation model

TABLE I

## PROPELLER FORCES - ECOLOGICAL TANKER

Type	Magnitude	Phase Angle
BEARING FORCES (LOADING EFFECT) BLADE RATE		
Alternating Thrust	10,062. lbs.	66.95°
Alternating Torque	387,200 in.lbs.	-112.78°
Vertical Force	3,128.4 lbs.	30.33°
Vertical Moment	1,080,000 in. lbs.	54.26°
Horizontal Force	8,837.8 lbs.	102.50°
Horizontal Moment	3,130,000	103.58°
VERTICAL SURFACE FORCES BLADE RATE		
Non-Cavity Loading Effect	3,825.2 lbs.	-141.05°
Non-Cavity Thickness Effect	537.4 lbs.	39.17°
Cavitation Thickness Effect	6,624.7 lbs.	18.68°
Total	3,734. lbs.	0.98°
VERTICAL SURFACE FORCES 2x BLADE RATE		
Cavitation Thickness Effect	3,028.75 lbs.	13.16°

forces must be accurately determined because the phase angle plays an important role in the overall structural response, as will be discussed later.

### Buoyancy Springs

The effect of the buoyancy of the water on the ship can be simulated by introducing vertical springs whose stiffnesses are equivalent to the buoyancy effects at the corresponding ship stations. Each node located along the wetted surface of the ship represents the free end of an axial bar, acting as a

column, which is the computer model equivalent of the buoyancy spring.

The equivalent vertical buoyancy stiffness at a ship station for a given draft is the vertical force necessary to produce a unit vertical deflection at that station. This stiffness,  $K_i$ , can be approximated as

$$K_i = DB_i L_i \quad (1)$$

where  $K_i$  = vertical buoyancy stiffness at station  $i$

$D$  = density of water

$B_i$  = breadth of ship at waterline at station  $i$

$L_i$  = station spacing at station  $i$ , taken as the average of the distance between stations  $i$  and  $i+1$  and the distance between stations  $i$  and  $i-1$ .

The stiffness of an axial bar acting as a column,  $K_B$ , is given by

$$K_B = \frac{A_B E_B}{L_B} \quad (2)$$

where  $A_B$  = cross-sectional area of the bar

$E_B$  = modulus of elasticity of the bar

$L_B$  = length of the bar

Equating the two stiffnesses,  $K_{Bi} = K_i$ , we get

$$A_{Bi} = \frac{L_{Bi} B_i D L_i}{E_{Bi}} \quad (3)$$

where the  $i$  subscript refers to station  $i$ .

The cross-sectional areas  $A_{Bi}$  are the total equivalent bar areas at each ship station. These areas are usually distributed to the various nodes in contact with water, in approximate proportion to an effective transverse width associated with each node.

### Hydrodynamic Added Masses

As the ship is vibrating, the fluid surrounding the ship hull produces an effect equivalent to a very considerable increase in the mass of the ship, known as "Added Mass". In ship vibration analysis, the added mass distribution should be properly taken into account since it is of the same order of magnitude as the mass of the ship.

The added mass distribution can be calculated by a computer program such as ABS/ADDMASS, which is based on linearized ideal fluid theory. The data per-

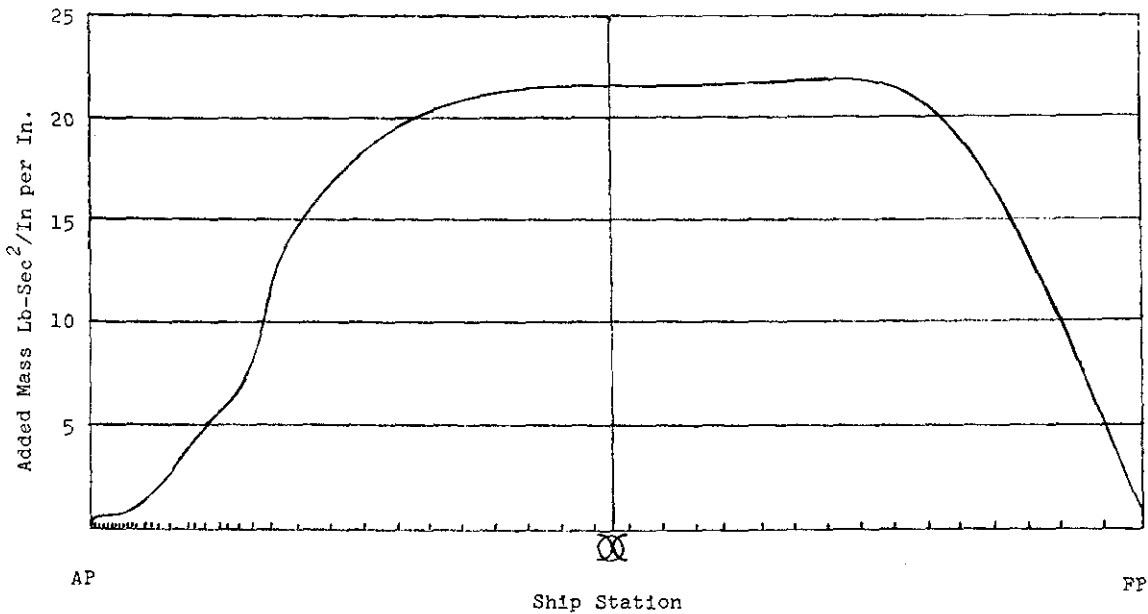


Fig. 5 Added mass distribution

taining to the hull geometry under water is needed in this calculation and the geometry is approximated by contour lines at various longitudinal stations. Each contour line is represented by line segments, on which an added mass distribution is found. A typical added mass distribution along the length of a medium-size tanker is shown in Figure 5.

As in the case of buoyancy springs, the total added mass per station is distributed to the various finite element model nodes in contact with water in approximate proportion to an effective transverse width associated with each node.

### Damping

The damping associated with ship hull vibration is relatively little known, but it is generally assumed that energy is dissipated by the following processes:

- a) Structural damping
- b) Cargo damping
- c) Water friction
- d) Pressure waves generation
- e) Surface waves generation
- f) Ship forward speed

The formulation of expressions for the damping forces poses a difficult problem that still requires extensive research. For practical purposes, however, it is assumed that the effects due to structural damping, cargo damping, water friction and pressure waves generation can be lumped together under the name of "internal" damping. Reference (1) presents a graph of the variation of this internal damping with frequency based on experimental data on all-welded ships. The effects of the generation of

surface waves and the forward speed can be called "hydrodynamic" damping and are usually calculated by computer programs such as "SEAKEEPING" (2). Within the frequency range of interest for ship vibrations, the internal damping increases with frequency in a logarithmic relation whereas hydrodynamic damping decreases asymptotically. At propeller blade frequencies, and higher, for example, the hydrodynamic damping is very small compared to the internal damping and can be neglected. Around the frequency of the hull girder lower modes, the hydrodynamic damping is usually predominant.

The damping values are usually converted to ratios of critical damping. These ratios are required to calculate the damping coefficients that must be used as input for computer programs that determine the forced response characteristics of a ship.

For a constant damping ratio for all frequencies, Rayleigh damping can be assumed and the damping matrix (C) can be expressed as

$$(C) = \alpha(M) + \beta(K) \quad (4)$$

where  $(M)$  = mass matrix  
 $(K)$  = stiffness matrix  
 $\alpha$  = mass damping coefficient  
 $\beta$  = stiffness damping coefficient

For a single degree of freedom system, the ratio of actual to critical damping  $\zeta$  can be expressed (3) as

$$\zeta = \frac{\alpha}{2\omega} + \frac{1}{2}\beta\omega \quad (5)$$

where  $\omega$  = frequency of mode under consideration.

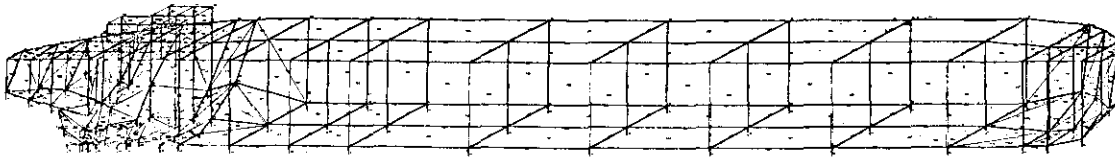


Fig. 6 Isometric view of oil carrier model - Port side

PROPELLER-INDUCED VIBRATIONS

Results on Selected Vessels

1100 ft. Oil Carrier. One vessel on which vibration characteristics and responses were investigated both analytically and experimentally was a 1100-ft. oil carrier. The entire ship was represented in the mathematical model, with one half actually modeled because of symmetry about the vertical centerline plane. This resulted in a model with 411 degrees of freedom. An isometric view of the model is shown in Figure 6.

The masses and structural stiffnesses define the free vibration characteristics of the mathematical model representing the ship. The summary of masses for the half ship modeled was:

MASSES (POUND SEC.<sup>2</sup>/INCH)

	FULL LOADING	BALLAST LOADING
Light Ship Equipment	5,493	5,483
Light Ship Structure	111,551	111,551
Cargo, Fuel, Ballast	767,493	304,396
Added Hydrodynamic	1,123,021	955,523
Total	2,007,548	1,376,953

The high relative magnitudes of the added hydrodynamic masses can be immediately noted from the above tabulation. Responses of the vessel to propeller-induced vibratory forces were calculated for the two loading conditions and 3 RPMs. The locations of the nodes and the corresponding deflection amplitudes are given in Table II.

870-ft. Ecological Tanker. Another vessel whose vibration characteristics and responses were thoroughly investigated analytically was a 870-ft. ecological tanker with double bottom and double skin (5).

A mathematical model of half the ship represented the entire ship because of symmetry, resulting in a model with 2605 degrees of freedom. The mathematical model is illustrated in Figure 7. Typical sections are shown in Figures 8, 9, and 10.

The responses of the vessel to propeller-induced vibratory forces were calculated for 2 RPMs at selected points, as listed in Table III.

833-ft. Great Lakes Bulk Carrier.

The vibration characteristics and responses of an 833-ft. bulk carrier were investigated both analytically and experimentally for two different stern configurations, one representing the ship as built and one incorporating a shroud or tunnel around the propeller (6).

As before, one half of the ship was used to represent the entire vessel, resulting in a model with 754 degrees of freedom. An isometric view of the model is shown in Figure 11.

The response amplitudes were calculated for two different propeller speeds and two different stern configurations (with and without tunnel) for approximately 60 points in the afterbody of the vessel. Table IV summarizes the response at 7 locations on the main deck, shown in Figure 12, where measurements were also taken for all four conditions.

Natural Frequencies. The lowest modes of free, undamped vibration of a ship are usually calculated to give an indication of the hull girder vibration characteristics. These are useful for checking the mathematical model by comparing the calculated hull girder frequencies with those obtained by relatively simple formulas, such as given in Reference (7). The lower modes are also of major importance in the study of wave-induced vibrations.

For the three vessels described, the lowest mode frequencies are summarized in Table V.

Typical mode shapes are shown in Figures 13 and 14. It can be seen from these mode shapes that the first mode corresponds basically to a heave motion, the second mode to a pitch motion and the third mode to a two-node deflected shape called the "springing" mode, representing the fundamental (lowest) mode deflection of a free-free beam. This third mode is sometimes referred to as the first or fundamental mode of vertical vibration (in which case it is possible to refer to the heave and pitch modes as the -1st and 0th modes respectively), and is the main mode of interest in the consideration of wave-induced "springing".

The higher modes represent local vibrations and must be understood as representing the response of a three-dimen-

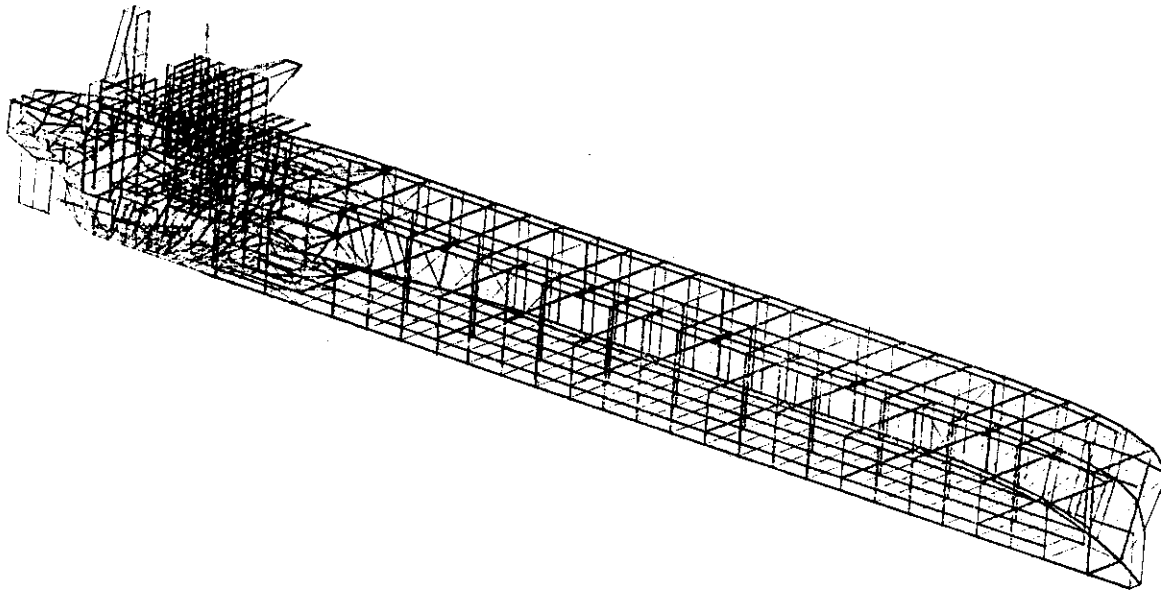


Fig. 7 Isometric view of ecological tanker model - Port side

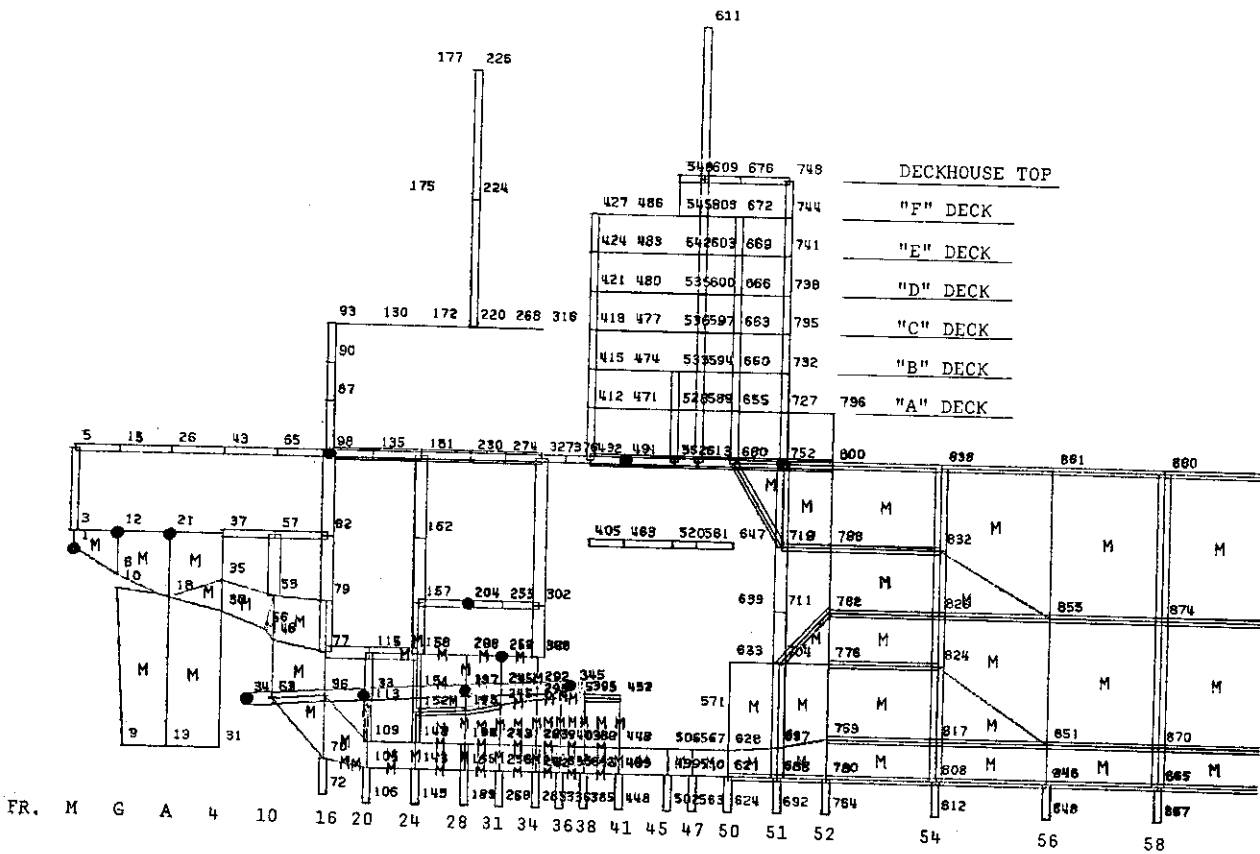


Fig. 8 Afterbody centerline - Ecological tanker

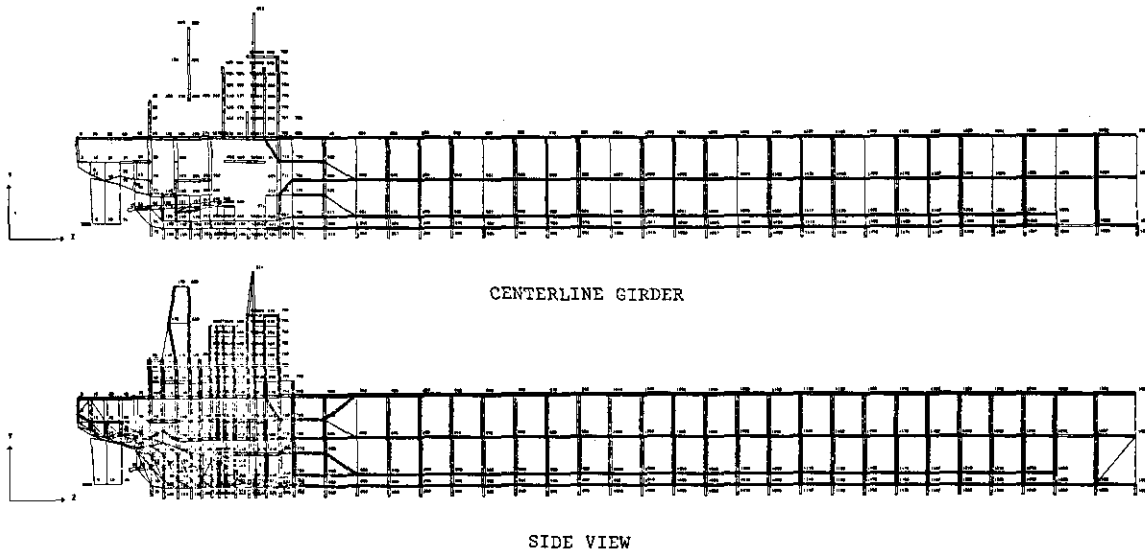
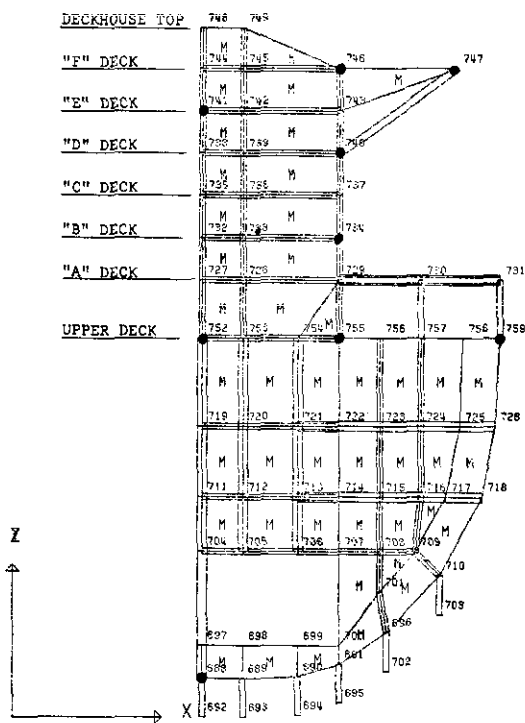


Fig. 9 Longitudinal sections - Ecological tanker



MODEL FR. 18 (SHIP FR. 51)

Fig. 10 Transverse frame in way of bridge wing - Ecological tanker

sional finite element model as opposed to the usual free-free beam representation of the ship.

Parametric Effects

Effect of Propeller Bearing Forces.  
The magnitude and the phase angle of pro-

PELLER bearing forces have an important effect on the response of the vessel's afterbody when combined with the surface forces. In order to quantify the effect of each component of propeller forces, responses at a representative location on the aft main deck of a Great Lakes bulk carrier were calculated at full power (120 RPM) for two different stern configurations.

The calculated propeller forces and phase angles are listed in Table VI.

The vertical amplitudes of displacement from these forces were calculated at various points on the main deck afterbody. The calculations were done for four different combinations of surface and bearing forces, and the results are shown in Table VII.

These results underline the importance of the phase angle of the propeller forces, especially in regions of low vibration amplitudes. To illustrate this further, the response at twice blade rate at point J is plotted in Figure 15.

An interesting observation is that with equal bearing forces for both stern configurations, the combined calculated response for the stern configuration without tunnel is almost 3 times smaller, even though the calculated surface force is about 8 times larger. This is of course due to the effect of the force phase angles, which becomes significant in the calculation of responses of small magnitude.

Effect of Damping. The damping associated with the vibrational response of a vessel is very difficult to determine analytically. In the frequency range of propeller-induced vibrations, the response is not very sensitive to

damping variations except in the case of external forces near resonance with one of the higher natural modes of the structure.

The results of a study of the effect of damping variations on the afterbody response of a Great Lakes bulk carrier are summarized in Table VIII. For the propeller-frequency range of interest, damping was calculated to be approximately 1% of critical. This damping was incorporated in the solution of the steady-state response to calculated pro-

pellor forces by means of the NASTRAN program. A damping matrix proportional to the stiffness matrix was used in the equations of motion.

To quantify the effect of damping variations, analyses were performed with values of 5 times and 1/5 of the calculated 1% damping. The results in table VIII show that for this particular case, the very small damping results in a large increase in calculated response amplitudes at twice the propeller blade rate.

TABLE II  
PROPELLER-INDUCED DISPLACEMENTS - OIL CARRIER  
NUMBER OF BLADES = 6

Location (Deckhouse extends from Fr. 27 to Fr. 57)	Node No.	* Dir.	Calculated Amplitude in Mils					
			85 RPM		82 RPM		70 RPM	
			Full Load	Ballast	Full Load	Ballast	Full Load	Ballast
Main deck $\perp$ Fr. 57	135	V	1.95	3.38	1.55	2.83	1.82	3.10
	135	L	0.85	1.68	0.75	0.95	0.64	0.94
Main deck off $\perp$ Fr. 57	136	V	1.93	3.45	1.48	2.91	1.67	3.31
Main deck, house edge Fr. 57	137	V	1.86	3.22	1.45	2.67	1.67	2.88
Deckhouse top $\perp$ Fr. 57	145	V	1.98	3.37	1.47	2.81	1.73	3.25
	145	L	2.07	3.10	1.54	2.10	1.40	3.46
Deckhouse top off $\perp$ Fr. 57	146	L	2.02	3.04	1.52	2.06	1.38	3.40
Deckhouse top,house edge Fr.57	147	L	2.00	3.00	1.51	2.03	1.37	3.37
Deckhouse top,house edge Fr.43	189	L	2.00	3.00	1.50	2.03	1.37	3.35
Inner bottom $\perp$ Fr. 40	196	V	3.13	6.01	2.97	5.71	2.35	4.21
Inner bottom at shell Fr. 40	197	V	2.62	5.07	2.65	4.87	2.27	4.07
Shaft $\perp$ , bull gear	199	V	2.91	5.72	2.67	5.48	2.27	4.22
	199	L	2.74	3.76	3.48	3.41	2.22	2.21
Inner bottom $\perp$ Fr. 37	207	V	2.71	5.68	2.67	5.50	2.38	4.70
Inner bottom at shell Fr. 37	208	V	2.23	4.75	2.25	4.67	2.22	4.40
Main deck, house edge Fr. 37	216	V	3.08	3.67	2.10	3.15	2.06	3.23
Deckhouse top $\perp$ Fr. 33	227	L	2.09	3.12	1.51	2.09	1.40	3.47
Deckhouse top off $\perp$ Fr. 33	228	L	2.09	3.15	1.45	2.05	1.40	3.45
Shaft $\perp$ , thrust bearing	229	V	2.88	6.41	2.83	6.07	2.26	4.62
	229	L	2.67	3.70	3.42	3.38	2.20	2.19
Inner bottom $\perp$ Fr. 30	238	V	2.72	3.70	2.24	3.75	1.90	4.78
Inner bottom at shell Fr. 30	239	V	3.01	3.63	2.50	3.68	1.90	4.75
Inner bottom $\perp$ Fr. 27	258	V	3.17	3.54	2.63	3.29	1.93	4.82
Inner bottom at shell Fr. 27	259	V	3.24	3.63	2.70	3.25	1.95	4.78
Main deck $\perp$ Fr. 27	266	V	4.03	4.12	3.61	3.07	2.12	4.44
	266	L	1.12	3.13	1.36	1.90	1.84	1.45
Main deck off $\perp$ Fr. 27	267	V	4.01	4.23	3.33	3.30	2.03	4.60
Deckhouse top $\perp$ Fr. 27	270	V	4.13	4.13	3.40	3.21	2.00	4.63
	270	L	1.24	2.69	1.10	1.50	1.18	2.38
Deckhouse top off $\perp$ Fr. 27	274	L	1.09	2.72	1.02	1.47	1.18	2.36
Shaft $\perp$ , line bearing	276	V	3.28	3.72	2.70	3.09	2.07	4.82
	276	L	3.65	4.41	4.20	4.01	2.27	2.81
Inner bottom $\perp$ Fr. 24	286	V	3.45	4.01	2.85	2.88	2.22	4.86
Inner bottom at shell Fr. 24	287	V	3.35	4.01	2.81	2.90	2.16	4.82
Shaft $\perp$ , Stern tube bearing	296	V	3.09	4.64	3.49	3.76	2.38	4.78
	296	L	4.25	4.81	4.62	4.37	3.07	3.16
Propeller centroid	305	V	3.49	4.90	3.57	3.87	2.57	4.87
	305	L	4.58	5.01	4.82	4.57	3.23	3.33

\* V = Vertical  
L = Longitudinal

The effects of damping variations cannot be generalized because these effects will depend on overall or local resonance conditions. Several studies (8), (9), have addressed this question and present useful information about the effects and importance of damping on ship response.

Habitability Criteria

There is a wide range of opinions concerning the acceptable levels of vibration on a ship. In general, vibration will cause physical annoyance to the crew before it adversely affects the ship

structure, machinery, equipment or cargo. The question of how much human beings can endure aboard ship has been the subject of many studies, but there is no general agreement on vibration acceptability criteria at this time.

The International Standards Organization (ISO) has recommended acceptable levels of vibration displacements for 8-hour fatigue-decreased proficiency as shown in Figure 16 (10). The ISO also suggests that different levels of human response to vibration for different exposure times can be obtained by ratios given in Table IX.

TABLE III  
PROPELLER-INDUCED DISPLACEMENTS - ECOLOGICAL TANKER  
NUMBER OF BLADES = 5

Location (Deckhouse extends from Fr. 16 to Fr. 52)	Node No.	Calculated Amplitude in Mils			
		Vertical		Longitudinal	
		93.7 RPM	85 RPM	93.7 RPM	85 RPM
Shell bottom $\angle$ stern	1	20.31	32.06		
Steering gear flat $\angle$ Fr. G	12	15.66	25.41	2.10	3.83
Steering gear flat $\angle$ Fr. A	21	9.66	16.83		
Propeller centroid	34	110.66	193.97	7.85	12.70
Stern tube, aft end	51	9.32	13.39	3.43	1.94
Bottom shell $\angle$ Fr. 16	70	3.47	2.74		
Upper deck $\angle$ Fr. 16	98	3.67	1.88	3.30	5.44
Upper deck at side Fr. 16	103	2.41	1.77		
Shaft $\angle$ line bearing	133	3.26	3.70		
Shaft $\angle$ thrust bearing	197	3.27	2.58	1.93	0.66
"C" deck at side Fr. 28	223	3.05	1.72	2.11	3.60
Deckhouse top $\angle$ Fr. 28	226	3.86	2.50	1.70	1.11
Engine room flat $\angle$ Fr. 31	248	2.81	2.40	2.85	2.37
Engine room flat off $\angle$ Fr. 31	250	6.54	4.60		
"A" deck side Fr. 31	265	3.08	1.82	1.96	3.54
Deckhouse top $\angle$ Fr. 34	323	3.27	2.22	4.03	4.76
Shaft $\angle$ bull gear	345	3.07	2.75		
Shafting foundation $\angle$ Fr. 36	347	3.23	2.73		
"D" deck side Fr. 36	369	2.84	1.92	2.98	4.21
Shafting foundation $\angle$ Fr. 38	395	3.12	2.78	1.81	0.68
39' Flat off $\angle$ Fr. 38	402	3.11	2.14	1.08	0.70
"E" deck off $\angle$ Fr. 38	425	2.65	1.89	3.50	4.53
Shafting foundation $\angle$ Fr. 41	452	2.82	2.91	1.88	0.72
Upper deck $\angle$ Fr. 41	491	2.40	1.76		
Inner bottom off $\angle$ Fr. 45	507	2.42	2.13		
Steering gear flat $\angle$ Fr. 45	520	2.87	1.93	1.31	2.00
"E" deck side Fr. 45	544	1.65	1.25	3.49	4.52
"C" deck $\angle$ Fr. 47	597	1.69	1.24	2.64	4.01
Deckhouse top $\angle$ Fr. 47	609	2.01	1.89	4.49	4.96
Top of mast $\angle$ Fr. 47	611	2.55	2.63	16.67	20.19
"C" deck side Fr. 50	665	1.50	1.18	2.65	3.99
Bottom shell $\angle$ Fr. 51	688	2.12	1.49		
"F" deck side Fr. 51	746	1.69	1.20	4.05	4.80
"F" deck wing edge Fr. 51	747	1.71	1.21	4.11	4.86
Upper deck at shell Fr. 51	759	1.18	0.94		
Shell bottom $\angle$ Fr. 25	922	2.14	1.55		
Shell bottom $\angle$ Fr. 92	1188	1.92	0.94		
Shell bottom $\angle$ Fr. 45	1295	2.99	0.92		

TABLE IV  
 PROPELLER-INDUCED DISPLACEMENTS - BULK CARRIER  
 NUMBER OF BLADES = 4

Node No. (Main Deck Aft.)	Point	Calculated Amplitude in Mils							
		120 RPM without tunnel		120 RMP with tunnel		110 RPM without tunnel		110 RPM with tunnel	
		B. R.	2xB. R.	B. R.	2xB. R.	B. R.	2xB. R.	B. R.	2xB. R.
559	L	4.47	0.52	3.38	0.55	3.17	0.31	2.17	0.42
542	B	3.77	0.39	2.87	0.43	2.75	0.20	1.89	0.33
502	F	0.26	0.14	0.14	0.30	0.26	0.25	0.20	0.21
472,442	H	0.25	0.13	0.20	0.27	0.25	0.28	0.18	0.13
442	K	0.15	0.13	0.17	0.21	0.37	0.17	0.28	0.02
503	A	1.25	0.17	0.92	0.28	1.22	0.05	0.84	0.06
471	J	1.50	0.22	1.03	0.61	1.41	0.14	0.96	0.07

B. R. = Blade Rate

TABLE V  
 CALCULATED NATURAL FREQUENCIES  
 (HERTZ)

Mode No.	1100-ft. Oil Carrier		870-ft. Ecological Tanker	833-ft. Bulk Carrier
	Full Load	Ballast	Ballast	Full Load
1	0.076	0.089	0.138	0.112
2	0.115	0.138	0.161	0.154
3	0.449	0.569	0.911	0.488
4	0.583	0.703	1.923	0.998
5	0.918	1.135	2.658	1.090
6	1.294	1.569	2.935	1.435
7	1.594	1.863	3.512	1.655
8	1.735	2.045	3.572	1.886
9	1.844	2.140	3.690	
10	2.066	2.310	3.999	

When vibrations occur in the vertical and horizontal directions simultaneously, the ISO recommends that the corresponding limits apply to each component and that the annoyance level be taken as the square root of the sum of the squares of the annoyance level associated with each component.

The preliminary guidelines proposed by SNAME HS-7 (Ship Vibration Panel) as presented in Figure 17 (11) show somewhat higher acceptable levels of vibration displacements. It is noted that the guidelines are to be used for both vertical and horizontal vibrations; in the low frequency range (0 to 4 Hz) human comfort is governed by horizontal vibration and above this range by vertical vibration.

Correlation of Measured and Calculated Data

A comparison between the calculated deflection amplitudes and the corresponding amplitudes measured during a sea-trial of a 1100-ft. oil carrier is presented in Table X.

The following comments apply to the comparison:

1. The ship region scrutinized is practically vibration-free and in this domain, even though the relative values are considerably different, they represent a consistently low magnitude. Simplifying assumptions introducing negligible inaccuracies in the overall analysis will tend to exaggerate the local differences at this low vibration level.
2. The mathematical model analyzed does not allow for representation of local structure, which may have some effect on vibration amplitudes.

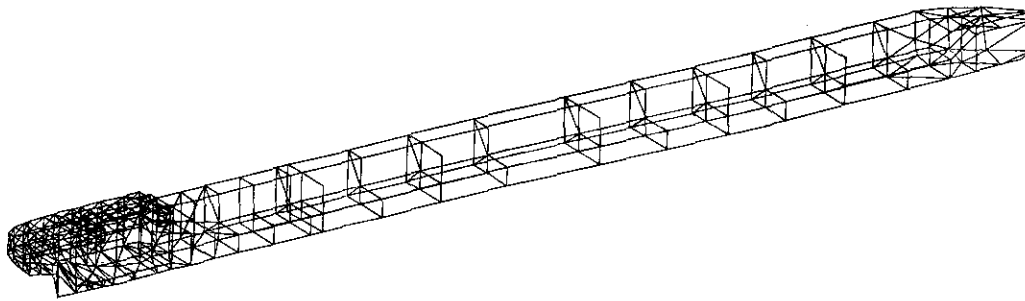


Fig. 11 Isometric view of bulk carrier model - Port side

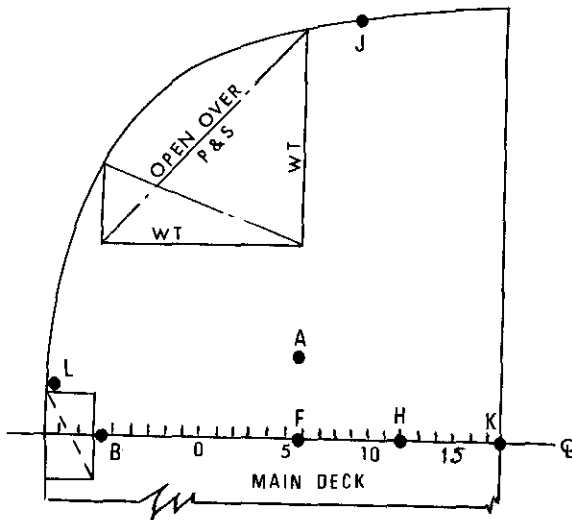


Fig. 12 Location of vibration measurements on main deck aft

3. One half of the ship was considered in the analysis, with the assumption of symmetry at the vertical centerline plane. The measured maxima, as given for the port and starboard sides in Table X, are not symmetrical.
4. The magnitude of the mean thrust, the time histories of the vertical and longitudinal alternating forces and their phase relationship were obtained from approximate design considerations. The corresponding actual values of these parameters are obviously somewhat different.
5. Many factors of ship operation which cannot be taken into account for the theoretical calculations are present during measurements. These include rudder movement (which was kept to a minimum but not zero value), uneven distribution of propeller forces on the hull, etc.

Considering the above-mentioned items, the correlation summarized in Table X is quite satisfactory and both the predicted and measured vibration levels are of a very low order of magnitude.

#### Discussion of Results

The illustrative examples for the three vessels analyzed indicate some general patterns of behavior such as the similar characteristics of hull girder lower modes and the maximum response of afterbody structure at propeller blade rate. Many of the results, however, cannot be predicted without a realistic finite element representation of the ship's afterbody and its solution by means of large-scale computer programs with dynamic capabilities. The complexity of the model and the scope of the analysis will of course depend on the severity of the vibration problems (expected or experienced). Special areas under investigation must be represented by a relatively fine-mesh model. The effects of parameters of doubtful magnitude must be carefully evaluated within their possible limits.

The presence and severity of ship-board vibration problems can best be ascertained by determining general trends and patterns of vibratory response, followed by a judicious selection of the predominant parameters and extrapolation of the pertinent data. A very helpful tool is the comparison with known vibration characteristics of similar ships.

The prevention of excessive vibration amplitudes can be accomplished by reducing the source of the exciting forces or by stiffening the local structure which may exhibit potential problems. The available options to do this diminish as the design and construction advance through their various stages; a preliminary indication of potential vibration problems is therefore highly desirable because a fairly large choice of solutions exists at an early design stage.

The exciting forces can be reduced by choosing a propeller with an optimum combination of characteristics, the most important of which are the number of blades, degree of skew and presence of ducts. The stern configuration around the propeller will also have a significant effect on the exciting forces, which can be decreased by factors such as a stern tunnel, stern fins or increased clearance around the propeller.

Modification of the ship structure will result in changes of stiffness, which in turn change the natural frequencies and the degree of resonant or near-resonant response amplitudes. A significant change in the stiffness of the entire hull girder can only be obtained with massive changes in the ship's shell, deck and longitudinal structure; the impracticality of doing this makes the hull girder stiffnesses (and, by extension, natural frequencies) fairly constant once the basic structural design is finished. On the other hand, local stiffnesses and frequencies can be modified with some judicious changes in local

structure or additions of structural members. Areas of the vessel's afterbody, especially deckhouses and engine room foundations, may experience excessive vibrations and can be strengthened accordingly.

#### WAVE-INDUCED SHIP HULL VIBRATIONS

##### Definition of Problem

At frequencies lower than those of propeller-induced vibrations, the ship vibrates in beam-like modes due to the excitation of waves. These vibrations are particularly important in large ships characterized by low natural frequencies and in fast ships of relatively high frequencies of encounter. A significant hull girder bending may occur due to the excitation of the beam-like low mode vibrations of the ship by the energy present in the corresponding frequency range of the sea spectrum. For this reason, it is necessary to consider the wave-induced vibrations in addition to the traditional aspects of ship design.

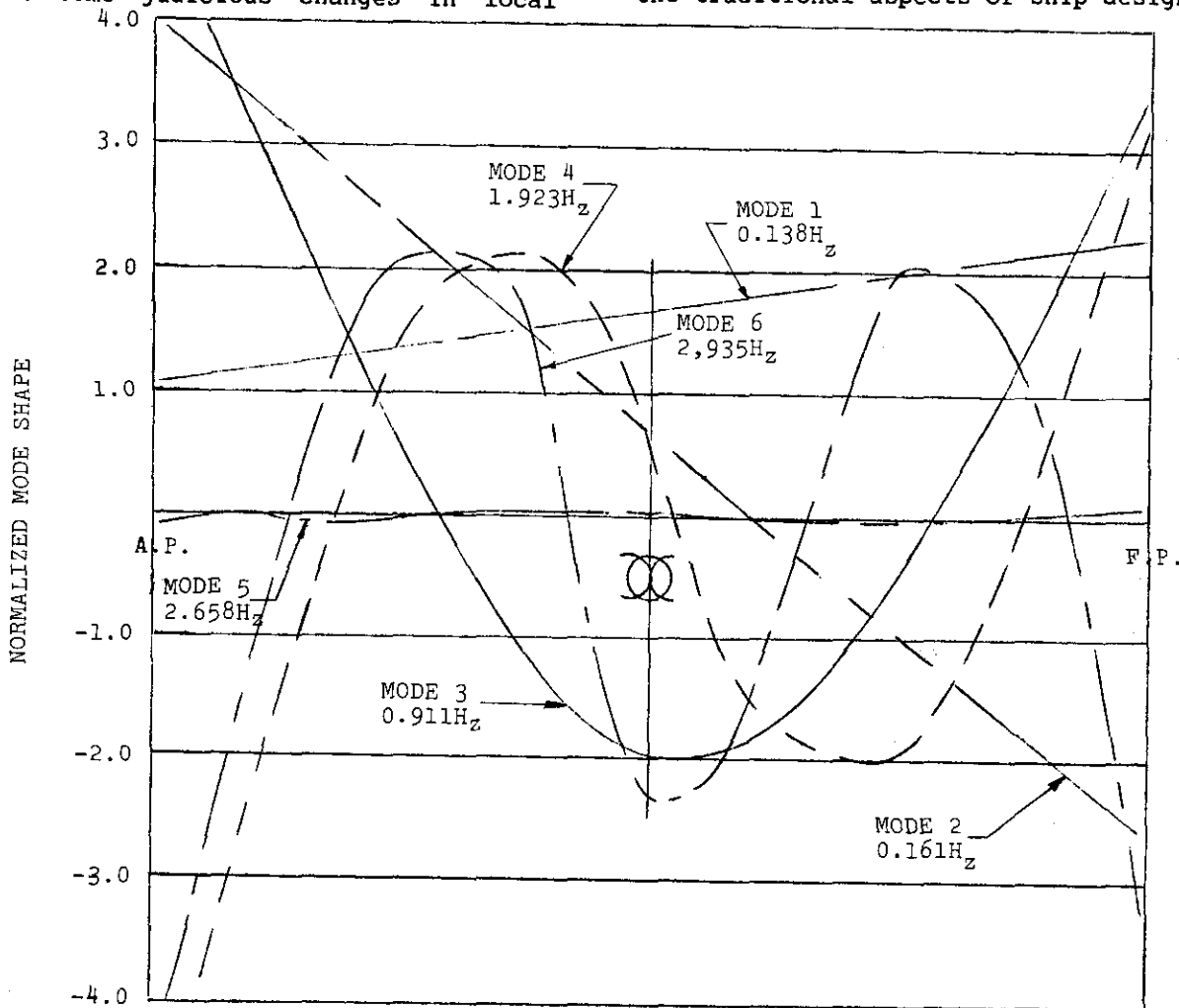


Fig. 13 Hull girder vibration mode shapes and frequencies - Ecological tanker - Modes 1 through 6

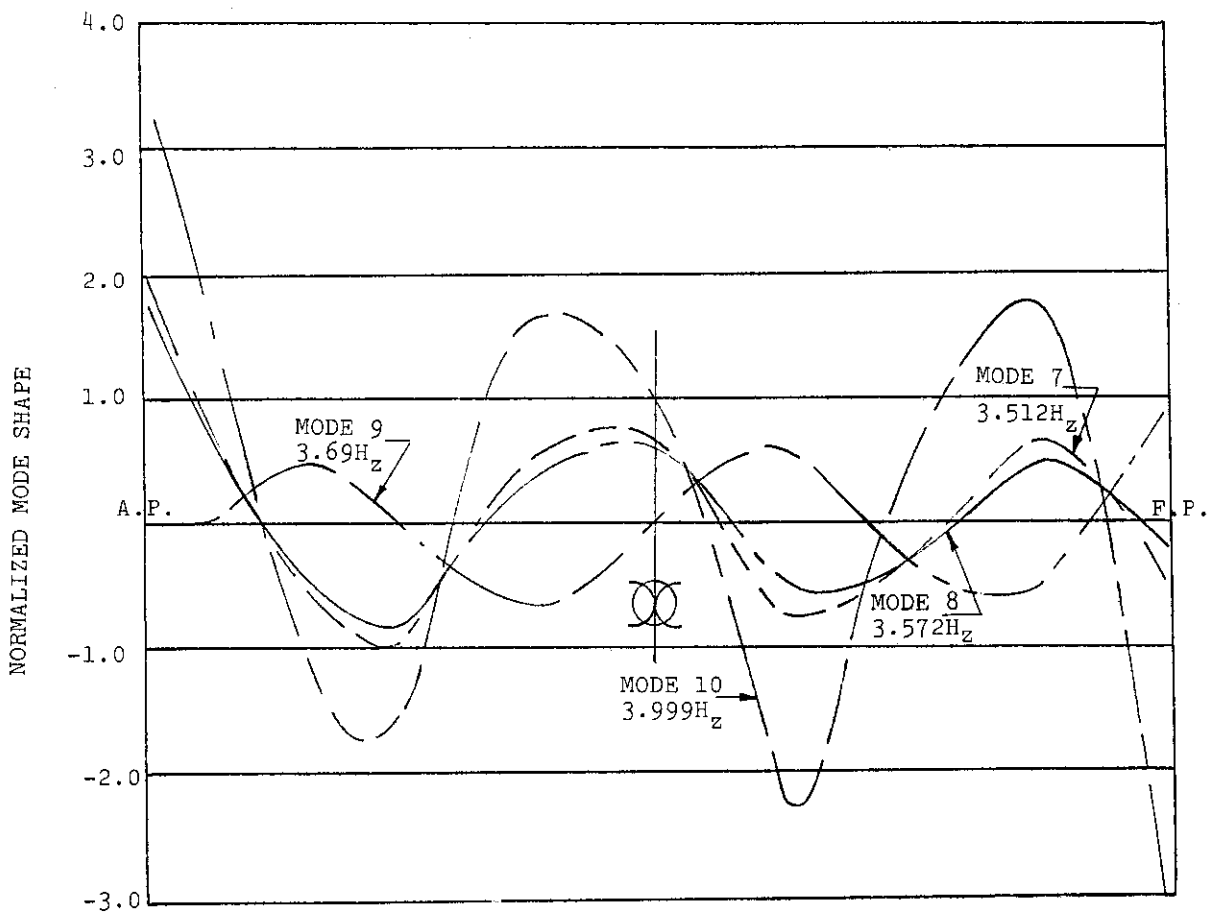


Fig. 14 Hull girder vibration mode shapes and frequencies - Ecological tanker - Modes 7 through 10

TABLE VI  
CALCULATED PROPELLER FORCES - BULK CARRIER

	with tunnel		without tunnel	
	B.R.	2xB.R.	B.R.	2xB.R.
1. Vertical Surface Force (lbs.) Phase Angle (°)	19,560. 90.41	3,841. 140.78	46,252. 50.25	30,769. -139.17
2. Vertical Bearing Force (lbs.) Phase Angle (°)	815. 133.21	766. -2.41	815. 133.21	766. -2.41
3. Longitudinal Bearing Force (lbs.) Phase Angle (°)	7401. -39.6	3141. 176.81	7401. -39.6	3141. 176.81
4. Bearing Bending Moment (in. lbs.) Phase Angle (°)	854,918. -63.21	279,776. -156.03	854,918. -63.21	279,776. -156.03

E.R. = Blade Rate

TABLE VII

EFFECTS OF PROPELLER-INDUCED FORCE COMPONENTS  
ON RESPONSE OF MAIN DECK AFT - BULK CARRIER

Point	Calculated Amplitude in Mils															
	120 RPM without tunnel								120 RPM with tunnel							
	1		1+2		1+2+3		1+2+3+4		1		1+2		1+2+3		1+2+3+4	
	B.R.	2xB.R.	B.R.	2xB.R.	B.R.	2xB.R.	B.R.	2xB.R.	B.R.	2xB.R.	B.R.	2xB.R.	B.R.	2xB.R.	B.R.	2xB.R.
L	3.46	.33	3.47	.31	3.60	.60	4.47	.52	1.55	.03	1.56	.04	2.13	.41	3.38	.55
B	2.92	.16	2.92	.15	3.04	.39	3.77	.39	1.31	.02	1.32	.02	1.82	.35	2.87	.43
F	.18	.33	.18	.32	.26	.32	.26	.14	.08	.03	.08	.04	.13	.02	.14	.30
H	.17	.31	.17	.30	.22	.28	.25	.12	.08	.03	.08	.03	.13	.07	.20	.27
K	.02	.09	.02	.08	.18	.08	.15	.13	.01	.01	.01	.01	.20	.15	.17	.21
A	.98	.12	.98	.11	1.00	.08	1.25	.17	.44	.01	.44	.01	.55	.19	.92	.28
J	1.23	.43	1.23	.41	1.21	.15	1.50	.22	.55	.04	.55	.04	.56	.34	1.03	.61

B.R. = Blade Rate

1 = Vertical surface force  
 2 = Vertical bearing force  
 3 = Longitudinal bearing force  
 4 = Bearing bending moment

TABLE VIII

## CALCULATED VERTICAL VIBRATION AMPLITUDES (MILS)

## BULK-CARRIER

Point	Blade Rate						Twice Blade Rate					
	with tunnel			without tunnel			with tunnel			without tunnel		
	Damping (Percent of Critical)											
	0.2%	1%	5%	0.2%	1%	5%	0.2%	1%	5%	0.2%	1%	5%
L	3.66	3.38	2.83	4.76	4.47	3.86	2.02	0.55	0.40	1.60	0.52	0.47
B	3.10	2.87	2.42	4.01	3.77	3.29	1.71	0.43	0.26	1.33	0.39	0.31
F	0.10	0.14	0.27	0.22	0.26	0.43	0.38	0.30	0.27	0.12	0.14	0.31
H	0.23	0.20	0.18	0.29	0.25	0.28	0.61	0.27	0.19	0.37	0.13	0.22
K	0.23	0.17	0.09	0.21	0.15	0.17	0.74	0.21	0.07	0.56	0.13	0.07
A	0.94	0.92	0.87	1.27	1.25	1.21	1.19	0.28	0.09	0.89	0.17	0.06
J	1.01	1.03	1.02	1.49	1.50	1.48	2.29	0.61	0.22	1.64	0.22	0.11

Large vessels operating in the Great Lakes represent a class of ships in which these wave-induced vibrations are, in general, more important than in ocean-going ships. The conditions necessary

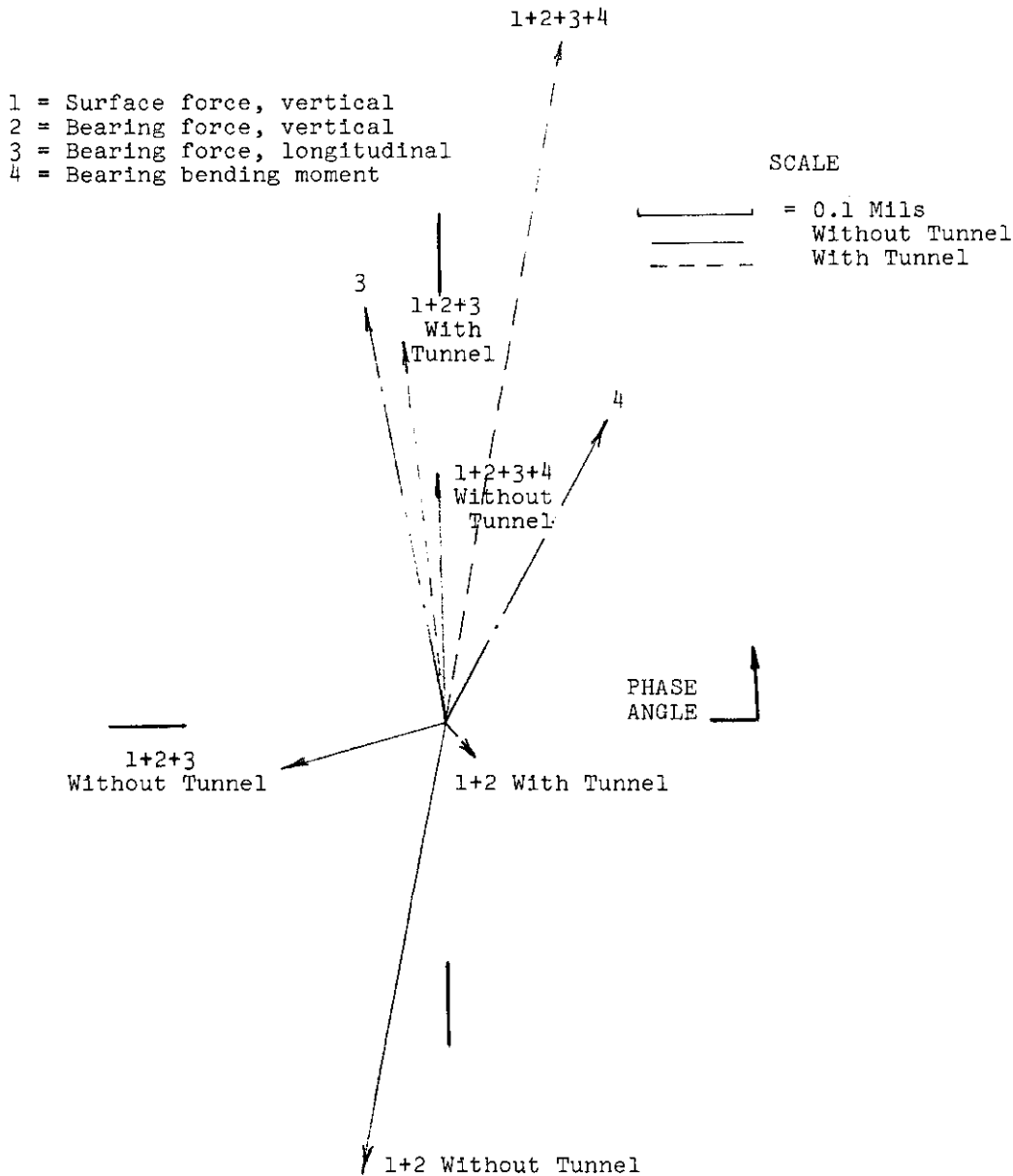
for so-called "springing" are set up by the relatively high flexibility and small draft of Great Lakes ships. In addition, the relatively low sea states of the Great Lakes increase the ratio of the springing moment to the wave loading moment.

The recent growth in ship length indicates a trend towards longer ships in the Great Lakes, while the width and depth are restricted by the physical confinement of the passageways. The increase in slenderness and the accompanying decrease in natural frequencies point out the need for taking the phenomenon of springing into consideration. Consequently, an extensive research program was initiated several years ago covering a broad spectrum of subjects which included Great Lakes wave behavior, instrumentation of ships, full-scale measurements of dynamic ship responses, model tests, data correlation, theoretical analysis, computer program

development, and the investigation of the effects of springing on fatigue strength. While the research work is continuing, some analytical results of the wave-induced dynamic responses together with correlation with full-scale measured data have been obtained.

Analytical Investigations and Computer Programs

Beam theory has long been successfully used to predict primary stresses in a ship due to hull girder bending. In the last two decades, a more accurate estimation of such stresses has been ob-



120 RPM-TWICE BLADE RATE-POINT J

Fig. 15 Vertical displacements for individual and combined propeller force components

TABLE IX

ANNOYANCE LEVELS REFERRED TO 8-HR.  
FATIGUE-DECREASED PROFICIENCY

Length of Exposure	Level of Severity		
	Reduced Comfort	Fatigue- Decreased Proficiency	Safe Exposure Limit
24 hr.	0.0795	0.25	0.50
8 hr.	0.318	1.	2.
4 4 hr.	0.53	1.68	3.36
2.5 hr.	0.72	2.25	4.5
1 hr.	1.19	3.75	7.5
25 min.	1.81	5.7	11.4
16 min.	2.14	6.875	13.5
1 min.	2.82	8.90	17.8

tained using finite element methods. Unfortunately, difficulties in formulating the expressions for the randomly varying environmental loads encountered by a ship require further investigation. Furthermore, the coupling of the hull girder flexibility and the external hydrodynamic forces represents another obstacle in using refined structural methods for the analysis of wave-induced ship vibrations. Strip theory was used successfully to compute the motion of ships in regular waves but its applications were limited to rigid-body considerations only. The seakeeping programs were, by their nature, not able to predict wave-induced vibrations. In other words, the ship dynamics were assumed to be decoupled into rigid-body motions governed by external hydrostatic and hydrodynamic forces, and vibrational behavior due to the finite stiffness of the hull structure.

In the beam-like vibrations, the ship bends or twists, but in general the hull sections do not deform. The hull dynamic response to wave excitation, including rigid-body motions and hull girder deformations, can be integrated in the study of vibratory floating beams. Bishop (12) has shown that the complete hull dynamics of vertical motion can be treated by the integrated analysis. The concept was generalized by Robert (13) to include the hull dynamics in a horizontal plane where the hydrostatic forces act as an external torsional stiffness with respect to roll, which is generally coupled with yaw and sway motions. The basic formulation of the integrated coupled equations of motion follows closely the non-uniform Timoshenko floating beam analysis. A normal mode procedure was adopted in the solution with successive Laplace transforms in order to account for the strong coupling of the damping terms in the low-frequency modes. Such coupling of the normal modes due to damping allows for the transfer of energy from one mode to another.

The computer program SPRINGSEA II (Springing and Seakeeping II) was developed based on the integrated analysis of the hull dynamic response to wave excitation (14). The program calculates the low-frequency wave-induced and high-frequency springing responses, the bandwidth parameter which checks the applicability of the Rayleigh distribution (15) and the statistics of the combined bending moments or bending stresses.

The data needed by the program consists of the hull geometry, draft, mass distribution, bending and shear stiffness distributions, ship speeds and heading angles. For each combination of ship speed, heading angle and frequency of encounter, the computations of the hydrodynamic added-mass and damping coefficients, the free-vibration modes and

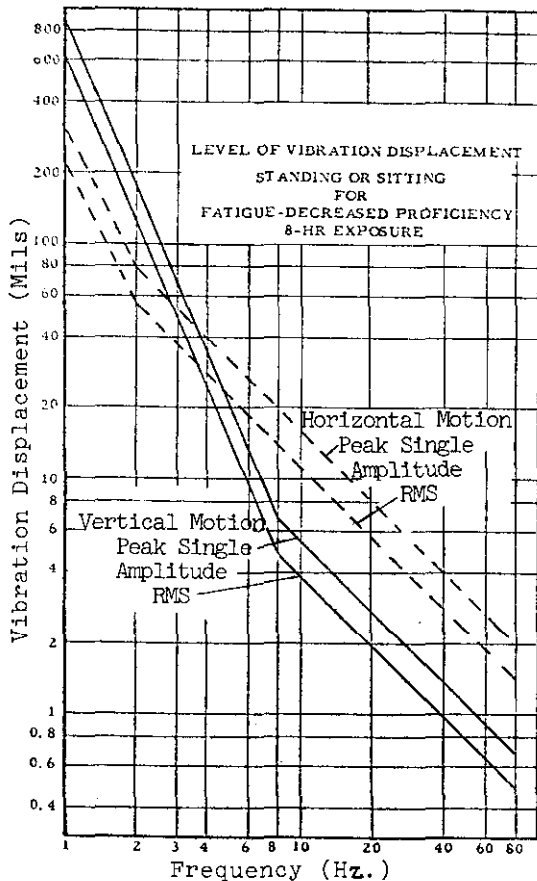


Fig. 16 ISO guide for evaluating human exposure to whole-body vibration

natural frequencies, the excitation forces, the forced vibrations and the response amplitude operator have to be repeated. One of the standard wave spectra built into the program can be used with an option which allows the user to specify his own spectrum as input data.

In the free-vibration analysis, the mass matrix is dependent on the frequency (and the speed of the ship) because of the added-mass contribution. At each hydrodynamic station the program computes the velocity potential, added mass, and damping coefficients for a large number of dimensionless frequencies. The results are stored in large arrays so that for a specific frequency of excitation, the hydrodynamic parameters can be accurately determined.

In the free-vibration analysis, the eigenvalue problem is solved for several frequencies so that the natural frequencies and normal mode shapes can be accurately interpolated for any frequency of encounter.

The program can accommodate ten different heading angles and over a hundred different frequencies of excitation. The large number of frequencies is required by the wide domain of interest when the high-frequency springing response is to be investigated. The peak resonance of this response is usually very sharp because of the small value of the associated damping, and a very small increment of frequency is required in order to correctly describe this peak. The response amplitude operator (RAO) is

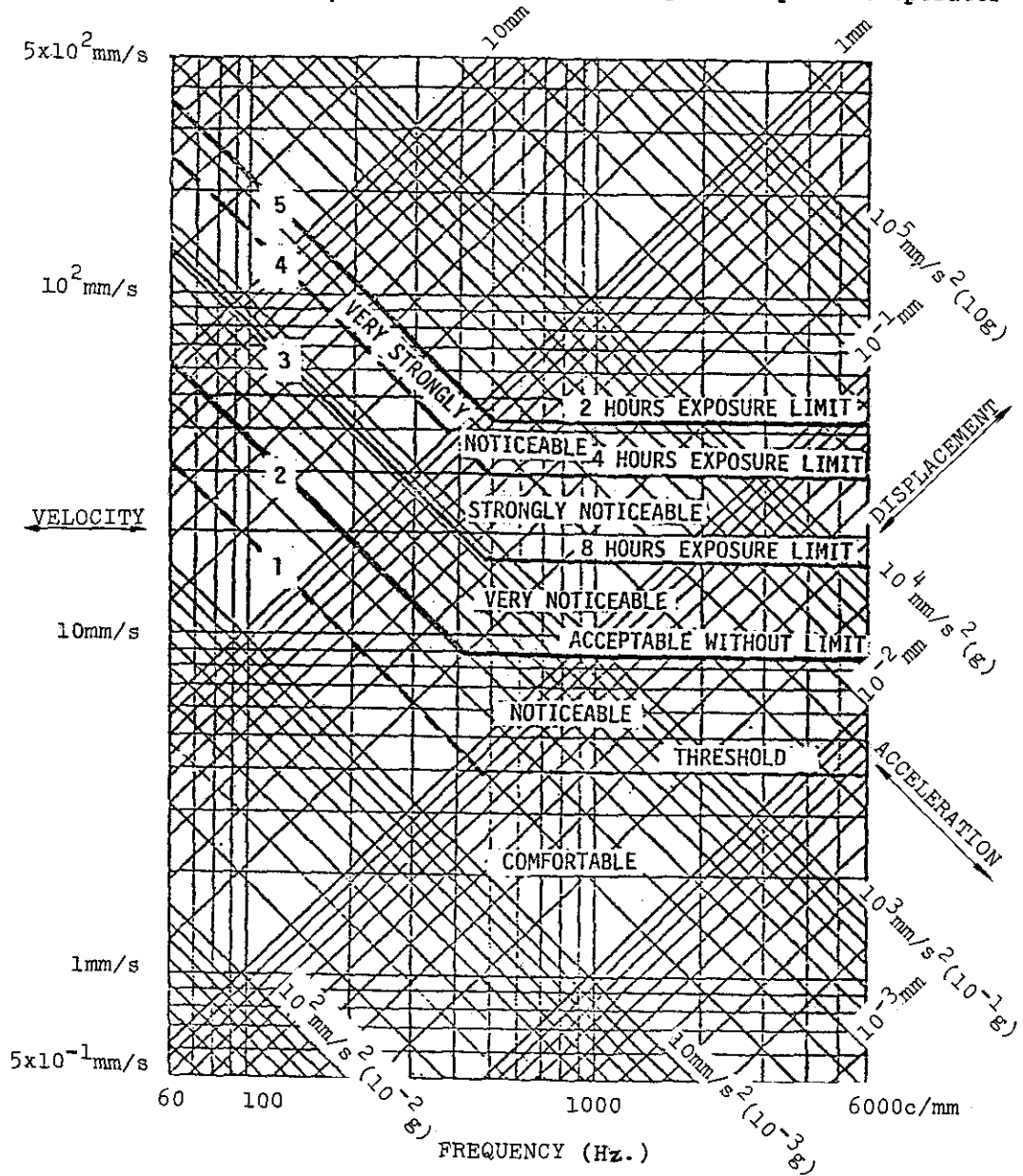


Fig. 17 Human exposure guidelines for vibrations on ships (vertical and horizontal)

TABLE X

## PROPELLER-INDUCED VIBRATIONS - OIL CARRIER

Node Location		Node No. P=Port S=Stb'd	Dir. *	Double Amplitude in Mils					
				85 RPM		82 RPM		70 RPM	
				Calc.	Meas.	Calc.	Meas.	Calc.	Meas.
Main Deck Frame 57 Forward Edge of Deckhouse	At $\phi$	135	V	0.58	0.96	0.39	0.92		
		135	L	1.45	1.33	1.23	1.10		
	Deckhouse Edge 36'-8" off $\phi$	137P	V	0.37	0.32	0.34	0.32		
		137S	V	0.37	0.39	0.34	0.78		
Nav. Bridge Deck Frame 57 Forward Edge of Deckhouse	At $\phi$	$\sim 145^a$	V	0.64 <sup>a</sup>	1.27	0.49 <sup>a</sup>	0.58		
		$\sim 145^a$	L	3.78 <sup>a</sup>	2.64	3.00 <sup>a</sup>	2.52		
	Deckhouse Edge 16'-8" off $\phi$	$\sim 146P^a$	L	3.72 <sup>a</sup>	4.64	2.96 <sup>a</sup>	2.96		
		$\sim 146S^a$	L	3.72 <sup>a</sup>	4.06	2.96 <sup>a</sup>	2.74		
Thrust Bearing	At Shaft $\phi$	229	V	2.33	1.65 <sup>b</sup>	2.79	1.84	1.85	0.60
		229	L	4.20	8.70 <sup>b</sup>	5.21	3.80	3.58	1.10
Main Deck Frame 26 Aft Edge of Deckhouse	At $\phi$	266	V	4.24	0.97	4.21	0.55		
		266	L	1.78	1.64	2.15	1.85		
	Deckhouse Edge 16'-8" off $\phi$	267P	V	4.73	0.35	3.02	0.82		
		267S	V	4.73	1.38	3.02	0.85		

a = Extrapolated

\*V = Vertical

b = Reading taken at 84 RPM

L = Longitudinal

TABLE XI

COMPARISON OF MAXIMUM STRESSES  
GREAT LAKES BULK CARRIERS

Ship	(H <sub>1/3</sub> ) max, ft.	C <sub>s</sub>	Type of Stress*	Maximum Stress, psi	Measured Maximum Stress, psi
Ford	23.5	0.819	c	23737	23000
			s	16270	16068
			w	19337	19097
Beeghly	23.5	1.012	c	28008	28000
			s	23968	22739
			w	16034	15272
Cort	23.5	0.781	c	33584	
			s	23711	
			w	26196	
	17.5	0.746	c	28484	29400
			s	20125	20306
			w	22140	18902

\*c = combined, s = springing,  
w = low-frequency wave-induced

computed for each heading angle and speed. The response spectrum is computed in the usual manner and the bandwidth parameter is calculated from the zero (variance), second and fourth moments of the spectrum. If a short-crested seas analysis is specified, the usual cosine-squared spreading function is used to distribute the energy in the long-crested wave spectrum with respect to the angular direction.

Comparison of Analytical and Measured Results

Most large slender ships operating in the Great Lakes experience wave-induced hull vibrations. An extensive test program involving a number of Great Lakes bulk carriers, sponsored by the American Bureau of Shipping and monitored by the U.S. Coast Guard, was carried out by Teledyne Material Research during the period 1972 through 1974, with one additional bulk carrier added in early 1975. The measurements on these ships consist primarily of midship deck bending stresses.

The top curve of Figure 18 shows a typical position of a recorded midship bending stress history. The recorded signals were passed through an automatic filtering system through which the high-

frequency and low-frequency stress response histories were separated as shown in the middle and bottom curves. The unfiltered, high-frequency and low-frequency stresses are identified as "combined", "springing", and "low-frequency wave-induced" stresses respectively. It should be noted that the combined stress does not include the static stillwater bending stress and that both the springing and low-frequency wave-induced stresses are wave-induced dynamic stresses.

Each of the three aforementioned types of stress history was utilized to produce a power spectrum from which the root-mean-square (RMS) values of the three types of stresses were computed. The spectra of the combined bending stress of two typical records are shown in Figure 19. The ordinates of the curves are not those of the actual power spectrum but the mean value of the spectral ordinate over a certain frequency range. Figure 19 illustrates two distinct patterns of wave energy allocation toward the peak of "low-frequency wave-induced" response and the peak of "springing". This process of energy allocation is controlled by the stage of wave development and is reflected in the value of the "peak frequency" of the associated wave spectrum.

Comparison between results obtained analytically and those computed from recorded data were carried out in two major ways, using the sample ships' short-term responses and their semi-long-term responses.

The short-term comparison is focused on the RMS values. The theoretical RMS values of the peak-to-trough combined springing and low-frequency wave-induced stresses of a given ship are computed with the significant wave height and scattering parameter  $C_s$  implicitly included in the theoretical wave spectrum. The RMS values of the recorded stress are obtained through integration of the response power spectra, filtered and unfiltered. An essential step for the wave height correction was carried out for data recorded on the "William C. Ford" and the "Charles M. Beeghly", including the determination of the scattering parameter as shown in Figure 20. The fact that the "Beeghly" data is highly concentrated indicates that only high stresses were recorded and the data is therefore biased. The "Ford" data, as well as the composite results, exhibit a widespread scatter.

The analytical results are weighed according to the actual percentage of occurrence of the relative wave heading angle. The resulting stress would be a function of the significant wave height only, for a given value of the scattering parameter. The weighed short-term RMS

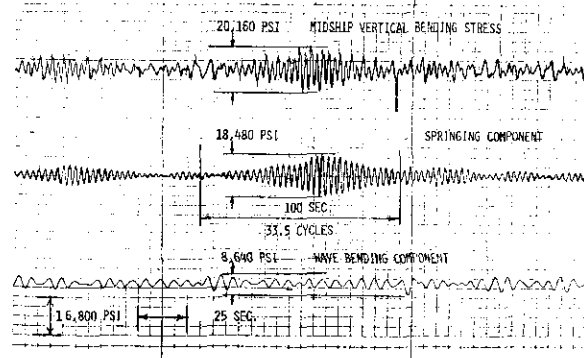


Fig. 18 Shipboard record of midship stresses-Great Lakes ore carrier - Storm condition

stress values of the "Beeghly" are shown in Figure 21, where it can be seen that the measured RMS stress values in the lower range of wave heights are higher than the theoretical curves. This behavior is attributed to the omission of the low stress records. At the higher end of the wave height scale, low stress is less probable and the records are therefore believed to be more complete. Moreover, the mean values fall into a relatively narrow range of the scattering parameter. The comparison also shows a trend of higher springing stress than low-frequency wave-induced stress in the low and intermediate sea-states, which is confirmed by both the analytical and measured results.

Similar comparisons for the "Ford" and the "Stewart J. Cort" are shown in Figures 22 and 23 respectively. Because of the high degree of scattering detected from the "Ford's" records, it is reasonable to assume that a similar situation prevails in the "Cort's" records. This observation is supported by the fact that the standard deviation of stresses within a sea-state group is unusually high compared with the corresponding mean value. The analytical curves shown in these two figures correspond to a scattering parameter  $C_s = 1$ . As  $C_s$  increases, the springing stresses increase and the low-frequency wave-induced stresses decrease. Therefore, the scattering phenomenon does not explain the fact that the measured RMS stress values are so low in the higher end of the wave height scale. A most likely source of discrepancy is believed to be the ship's lower speed in a stormy seaway, whereas the theoretical curve was computed based on a fixed design speed.

For the semi-long-term response, the approach is somewhat different from the usual mean value correlation. The objective is to produce a set of theoretical curves for the probability of the maximum stresses exceeding various stress levels. These curves are compared with their counterparts produced from

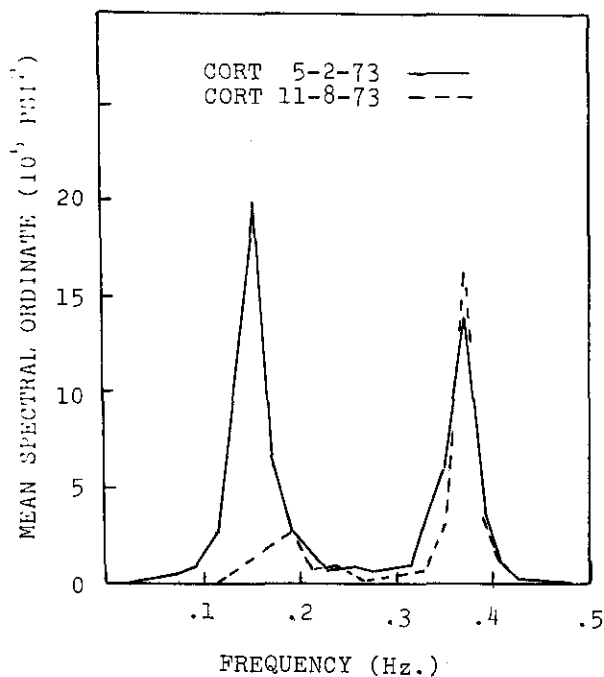


Fig. 19 Typical stress spectrum

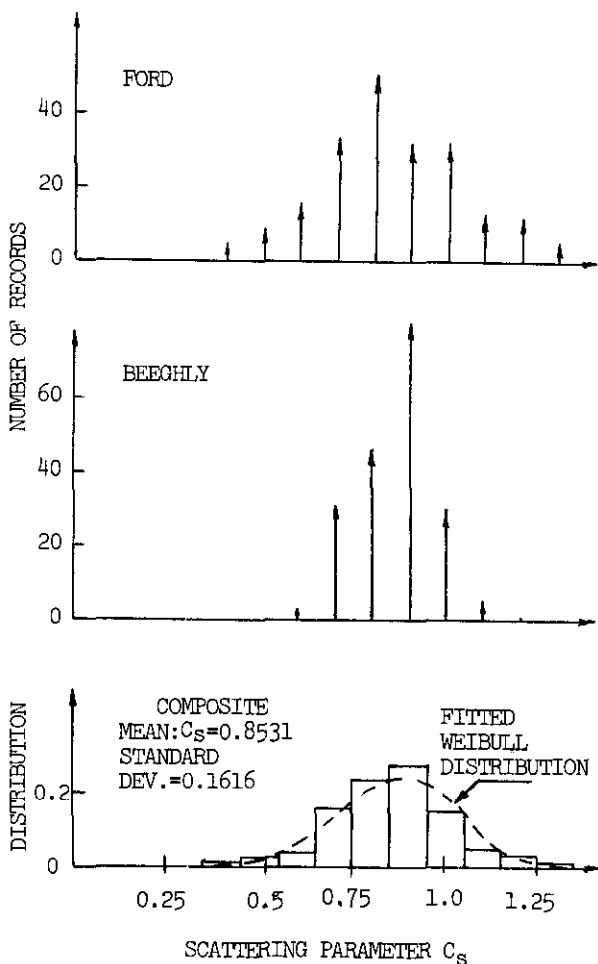


Fig. 20 Distribution of scattering parameter

the extreme measured RMS stress values of all sea-state groups. This type of correlation is pursued mainly for two reasons. The first reason is that the stress records are biased toward the higher values (low stress records were either omitted or discarded), especially in the case of the "Beeghly". Thus, the distributions of the Rayleigh parameter are completely distorted and the stresses based on all the stress records are higher than they should be. On the other hand, the omission of the low stress records does not affect the extreme RMS stress values. The second reason is that from the practical standpoint it is more useful to predict the extreme stress expectancy than the expected mean value.

For the sake of completeness, however, the resulting extreme stress curves, both theoretical and experimental, are also compared with the expected mean values obtained from all the stress records.

Figures 24 to 26 show the maximum peak-to-trough stresses versus  $\log(N)$ , where  $N$  is the number of stress records. The three types of stresses are staggered to improve clarity. The solid curves are computed analytically while the dash and dash-dot curves are computed using the extreme RMS values and the "complete" set of RMS values of the stress records, respectively. It is interesting to note that, in the cases of the "Beeghly" and "Ford", not only do the theoretical curves agree well with the "extreme" experimental curves, but both agree well with the highest stresses recorded. In the case of the "Cort", the theoretical curves are higher than those obtained from test data. It appears that a major cause of discrepancy is the error in the observed wave heights. Table XI also gives a comparison of the maximum stresses.

#### Discussion of Results

Based on the integrated analysis of hull dynamics, the coupled equations of a ship have been solved to determine the low-frequency wave-induced moments and the high-frequency vibratory loads. An analytical model was used in conjunction with the SPRINGSEA II program to predict the loads on several bulk carriers operating in the Great Lakes. The computerized model was calibrated using full-scale measurements taken onboard the vessels "Cort", "Beeghly" and "Ford". Long- and short-term comparisons between the calibrated computerized model and the full-scale measurements were made. The results of the comparisons were, in general, satisfactory.

In addition to the low-frequency wave-induced stresses, the importance of springing stresses has been recognized, particularly for the large bulk carriers

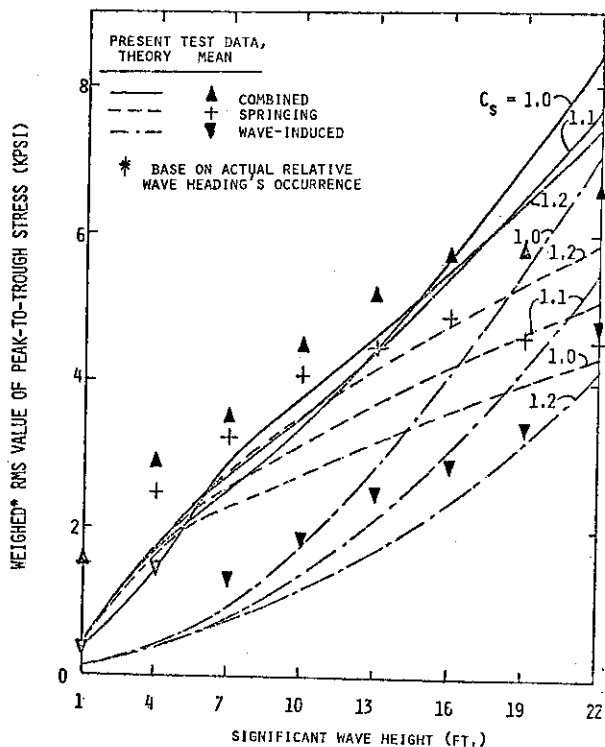


Fig. 21 Comparison between measured and theoretical stresses of the "Beeghly"

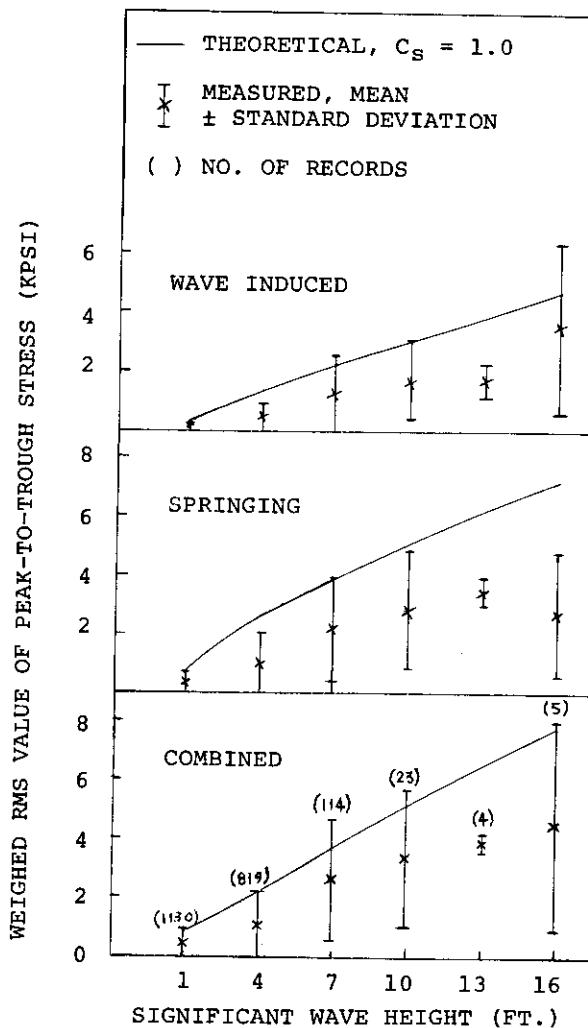


Fig. 23 Comparison between measured and theoretical stresses of the "Cort" operating in the Great Lakes.

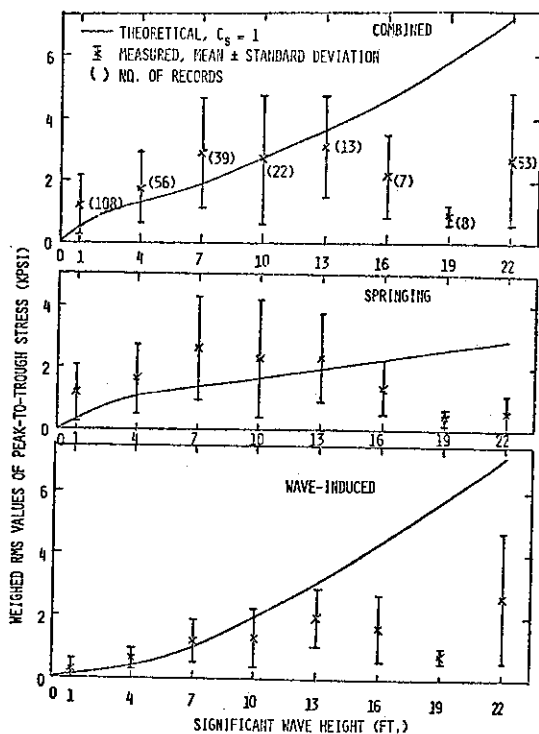


Fig. 22 Comparison between measured and theoretical stresses of the "Ford"

A simple illustration of the significance of springing is the percentage increase in the combined stresses due to springing. The resulting increases of the mean of the RMS values are 46.5, 51.5, and 57.4 percent for the "Ford", "Beeghly", and "Cort", respectively. Since the individual histograms are assumed to follow the Rayleigh distribution, it follows that the mean value of the maximum stress is proportional to the mean of the RMS values. Therefore, the preceding percentage increases can also serve as estimates based on maximum stresses.

The computerized analytical model was also used to investigate the effect of springing on the combined stresses. Such an effect depends to a large extent on the significant wave height, and, more importantly, on the stage of sea development as characterized by the peak frequency of the wave spectrum. The "Cort", for example, would experience an increase in the deck stresses due to

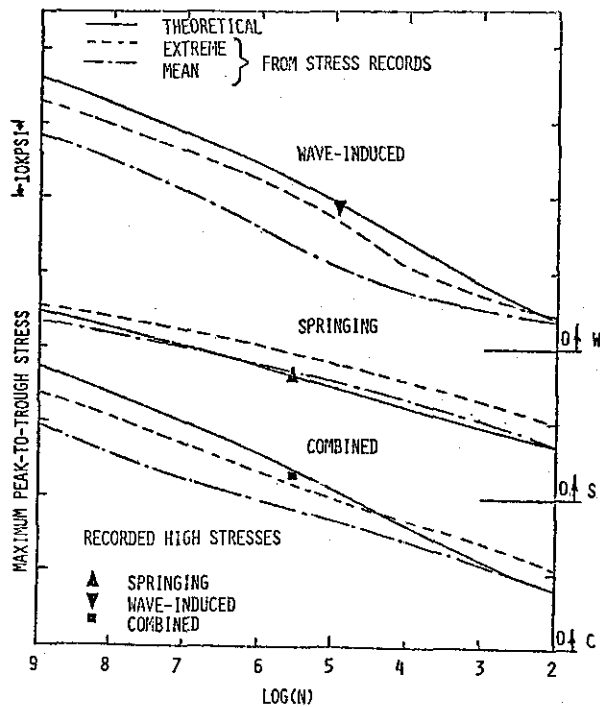


Fig. 24 Comparison between long-term recorded and theoretical stresses of the "Ford"

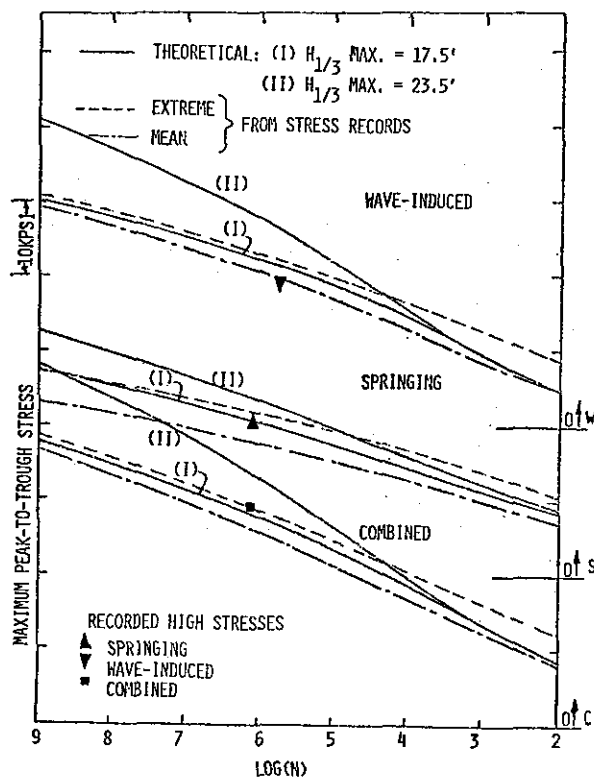


Fig. 26 Comparison between long-term recorded and theoretical stresses of the "Cort"

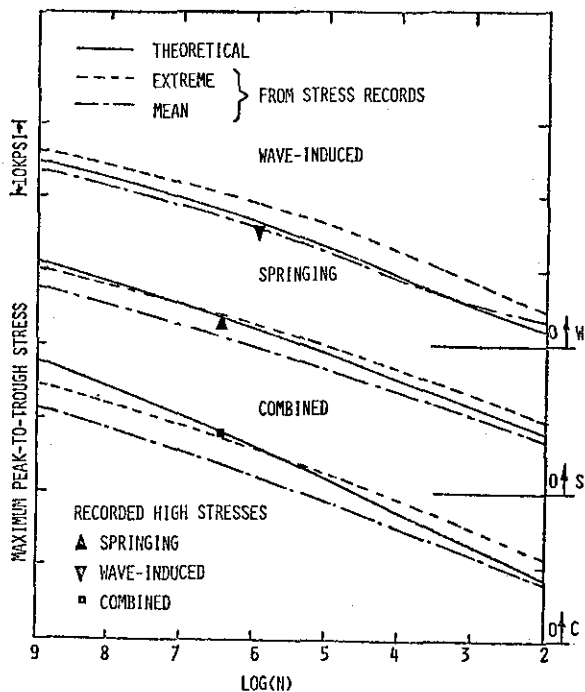


Fig. 25 Comparison between long-term recorded and theoretical stresses of the "Beeghly"

springing of about 10 percent in a fully developed sea with a significant wave height of 15 feet. On the other hand, in a developing sea condition characterized by the same significant wave height, such an increase would become 60 percent. In a severe sea condition with a significant wave height of 30 feet, which is probably

of more interest for design purposes, the increase in the combined stresses due to springing is about 6 percent. These figures should be compared with the 57.4 percent increase determined from the full-scale measurements. It should be noted, however, that most of the full-scale measurements were taken in the relatively low sea states which the ship had encountered.

It is of interest, therefore, to assess the importance of the springing loads as a portion of the total loading in the design of long Great Lakes bulk carriers. An increase should be expected in the total bending moment or stress due to springing, and this increase will affect the design section modulus of the hull.

#### CONCLUSIONS

The calculation of wave-induced vibrations on a vessel can usually be performed by using an elastic beam approximation, but finite element analyses provide the best available techniques for thorough investigations of propeller-induced vibrations or coupled effects. New developments and improvements in existing computer programs, such as dynamic condensation, provide more cost-effective solutions with a greater degree of confidence in the results. On-board measurements provide an indication of

the effect of simplifying assumptions made in the various parts of the analysis.

The analysis of wave-induced vibrations presented in the paper is a special type of random analysis, utilizing an energy spectrum and RMS values. The SPRINGSEA II program can also be used for the case of a general (non-sinusoidal) forced vibration, such as slamming.

The desirability of preventing vibration problems at an early design stage is obvious. Preliminary engineering calculations can indicate the best balance between an efficient, economical ship and propulsion system combination and a minimum level of shipboard vibrations. A significant change in hull girder natural frequencies to avoid resonance with forcing frequencies can only be accomplished by major changes in the ship's hull girder structure, which are difficult and impractical.

Vibrations can be reduced by reducing the exciting forces on the ship. This can be accomplished by changing the configuration of the stern around the propeller, (addition of stern fin or stern tunnel, increase of clearance, etc.) or by modifying the propeller itself (changing the number of blades, using a highly skewed or a ducted propeller, etc.). Vibrations can also be reduced by changing the natural frequencies of the ship structure to avoid resonant or near-resonant conditions. This can be accomplished for parts of the vessel by the judicious addition of structural members which will provide the necessary increase in local stiffness and frequency. Another proposed technique for reducing vibration responses is the use of auxiliary tanks with liquid and air masses which serve as vibration dampers.

Further research and investigation is definitely indicated in many of the areas discussed in the paper. Some of these areas are the calculation of propeller forces with the proper phase angles, damping and its distribution over the various natural modes of the ship structure, a more accurate derivation of the added mass as a function of frequency, etc.

#### ACKNOWLEDGEMENTS

The author wishes to acknowledge the valuable assistance of Mr. M. Wojnarowski and other members of the Research and Development staff at the American Bureau of Shipping in the preparation of this paper.

#### REFERENCES

1. R.A. Goodman, "Wave-Excited Main Hull Vibration in Large Tankers and Bulk Carriers", Trans. RINA, 1971.

2. "5-D Seakeeping Program", Massachusetts Institute of Technology, 1974.
3. W. Hurty and M. Rubinstein, "Dynamics of Structures", Prentice Hall, Inc., Englewood Cliffs, N.J., 1964.
4. American Bureau of Shipping, Research & Development Division, "Vibration Study of 265,000 DWT Oil Carrier", Technical Report RD-75001-1, July 1975.
5. American Bureau of Shipping, Research & Development Division, "Ship Hull and Propulsion System Vibration Analysis of Ecological Tanker", Technical Report RD-77011, July 1977.
6. W.S. Vorus, S.G. Stiansen and R.H. Bertz, "Correlations of Propeller-Induced Forces and Structural Vibratory Response of the M.V. Roger Blough", Department of Naval Architecture & Marine Engineering, University of Michigan, No. 193, October 1977.
7. F.H. Todd, "Ship Hull Vibration", Edward Arnold Ltd., London, 1961.
8. S. Hylarides, "Damping in Propeller-Generated Ship Vibrations", Netherlands Ship Model Basin, Publication No. 468, 1974.
9. G. Ward and G.T. Willshare, "Propeller-Excited Vibration with Particular Reference to Full-Scale Measurements", Trans. RINA, 1976.
10. F.E. Reed, "Acceptable Levels of Vibration on Ships", Marine Technology, April 1973.
11. "Ship Vibration and Noise Guidelines", Preliminary Proposal, SNAME HS-7 Panel, November 1976.
12. R.E.D. Bishop, R.E. Taylor and K.L. Jackson, "On the Structural Dynamics of Ship Hulls in Waves," Trans. RINA, 1973.
13. O.J. Robert, "Integrated Theory of Seakeeping and Structural Dynamics," M.S. Thesis, Department of Ocean Engineering, Massachusetts Institute of Technology, June 1975.
14. S.G. Stiansen, A.E. Mansour and Y.N. Chen, "Dynamic Response of Large Great Lakes Bulk Carriers to Wave-Excited Loads, Trans. SNAME, 1977.
15. S.G. Stiansen and A.E. Mansour, "Ship Primary Strength Based on Statistical Data Analysis", Trans. SNAME, 1975.